CHEMISTRY
A EUROPEAN JOURNAL

DOI: 10.1002/chem.200700148

Low-Temperature Adsorption/Storage of Hydrogen on FAU, MFI, and MOR Zeolites with Various Si/Al Ratios: Effect of Electrostatic Fields and Pore Structures

Sung Hwa Jhung,* Ji Woong Yoon, Ji Sun Lee, and Jong-San Chang*[a]

Abstract: Several zeolites, such as faujasite, mordenite, and ZSM-5, with various aluminum contents have been used to analyze the effect of aluminum or cation concentration (strength of electrostatic field) on hydrogen adsorption at low temperature. Irrespective of the zeolite structure, the adsorption capacity, isosteric heat of adsorption ($-\Delta H_{ads}$), surface coverage, and micropore occupancy increase with increasing aluminum content of a zeolite. Zeolites with a higher amount of aluminum favorably adsorb hydrogen at relatively low pressures. For zeolites with similar aluminum contents, the adsorption capacity, isosteric heat of adsorption, surface coverage, and micropore occupancy are in the order of mordenite > ZSM-5 > faujasite, probably due to differing pore sizes and the presence or absence of pore intersections. This work demonstrates that zeolites with strong electrostatic fields and narrow pores without intersections are beneficial for high hydrogen uptake.

Keywords: adsorption · aluminum · electrostatic field · hydrogen · zeolites

Introduction

Efficient storage of hydrogen is very important for the utilization of hydrogen, one of the best alternative fuels for vehicles powered with fuel cells.[1,2] The storage of hydrogen by adsorption, including physisorption, by using porous materials is one of several methods[3] currently being investigated. Porous materials, such as carbons,[4–6] aluminosilicate zeolites,[7,8] and inorganic–organic hybrid materials, such as metal-organic frameworks (MOFs),[9–13] have been studied as potential hydrogen sorbents. Materials with high porosity (expressed either in terms of surface area or pore volume) are invariably sought due to the general consensus that higher porosity leads directly to higher overall hydrogen uptake.[1,3,8,14] Very recently, adsorption capacity as high as 6.1–7.5 wt% has been reported by using high surface area MOFs[15–17] at liquid-nitrogen temperature.

Several strategies to increase the adsorption capacity, including 1) optimizing pore size,[18–21] 2) preparation of frameworks from light metal species,[18] 3) utilization of hydrogen spillover,[22] and 4) optimization of adsorption energy,[9] have been suggested. Optimum pore or small pore size is stated to be important to enhance the hydrogen uptake.[9] Very small pores lead to high binding affinity due to increased van der Waals contact area.[18] Effective use of the available pore volume is most likely in materials with smaller pores.[19] Hysteresis in hydrogen adsorption and desorption occurs in a very small pore which may not allow hydrogen to pass freely.[23] Very recently, we have demonstrated that aluminophosphate molecular sieves (AlPOs) with small pore show high adsorption capacity (per surface area or micropore volume) and heat of adsorption due to the increased interaction between the AlPOs (with small pore) pore walls and hydrogen.[20] Very recently, it has also been shown that catenation of a MOF, even with concurrent reduction of pore dimension, leads to a significant enhancement of hydrogen adsorption.[21,24] Light metals, such as magnesium, improve gravimetric hydrogen storage capacities by lowering the weight of the adsorbent.[18] Li and Yang have shown that the hydrogen storage capacity can be increased much with the idea of hydrogen spillover for adsorbents including a physical mixture of Pt/carbon and MOFs.[22]

Acid–base, electrostatic, and dipole interactions have also been considered to be important.[25,26] For example, Froudkis[26] has shown that high hydrogen adsorption on an alkali-

[a] Dr. S. H. Jhung, J. W. Yoon, J. S. Lee, Dr. J.-S. Chang
Research Center for Nanocatalysts
Korea Research Institute of Chemical Technology (KRICT)
P.O. Box, 107, Yusung, Daejeon 305–600 (Korea)
Fax: (+82) 42-860-7676
E-mail: sung@krict.re.kr
jschang@krict.re.kr

metal-doped carbon nanotube was due to the charge-induced dipole interaction between hydrogen and the alkali metal. Development of open or coordinatively unsaturated sites (CUS) of metal atoms is also helpful to increase the adsorption strength.[9,24,27–29] CUS in a MOF enhances the hydrogen adsorption capacity.[21] Some of us have reported that coordinatively unsaturated nickel sites of porous nickel phosphate[27] or nickel-5-sulfoisophthalate[28] leads to an adsorption of hydrogen with high heat of adsorption and hysterisis in adsorption–desorption isotherms.[27,28] Kazansky et al. have suggested that the hydrogen adsorption on faujasite zeolites is high when the faujasite has a low Si/Al ratio because there are more basic sites and stronger perturbation of the H–H bond.[25] However, recently, Langmi et al. reported that the hydrogen adsorption capacity does not rely on the Si/Al ratio but only on the BET surface area.[30] These observations suggest that the effect of Si/Al ratio or electrostatic field of a zeolite is an important parameter for hydrogen storage; however, this is not yet understood thoroughly.

In this work, the effect of the electrostatic field of porous materials on the hydrogen sorption properties, including adsorption capacity and energy etc. has been studied by using wide-ranging conditions, including zeolite structures (several important zeolites, such as faujasite (IZA code[31] FAU), mordenite (IZA code MOR), and ZSM-5 (IZA code MFI)), Si/Al or Si/Na ratios and temperatures. Moreover, the effects of pore structure, such as pore size and the presence of an intersection of zeolites (with similar Si/Al ratios), on the hydrogen adsorption has been examined.

Results

Figure 1 shows the adsorption isotherms at 77 K over the three zeolites with various Si/Al ratios. The desorption isotherms have the same characteristic lineshapes as the adsorption isotherms (data not shown) which represents fully reversible adsorption due to physisorption. As shown in Figure 1, the zeolites adsorb various amounts (71–172 mL g^{-1}) of hydrogen at 760 Torr depending on the structure and Si/Al ratio. The adsorbed hydrogen capacities are summarized in Table 1 and Figure 2, illustrating the monotonous increase of adsorption capacity with increasing aluminum (and sodium accordingly) concentration. This suggests the increase of interaction between hydrogen and the zeolite pore walls or sodium ions when the concentration of aluminum or sodium is high.

The isosteric heat of adsorption ($-\Delta H_{ads}$) can be calculated by using the Clausius–Clapeyron equation[32] from the isotherms at various adsorption temperatures. Figure 3 shows the typical isotherms over FAU (60) zeolite for various temperatures (77, 87, and 90 K). As is well known, the adsorbed hydrogen decreases when increasing the adsorption temperature. Other zeolites show very similar dependences on adsorption temperatures. Figure 4 illustrates the dependences between ln$P$ versus T^{-1} for the FAU zeolites

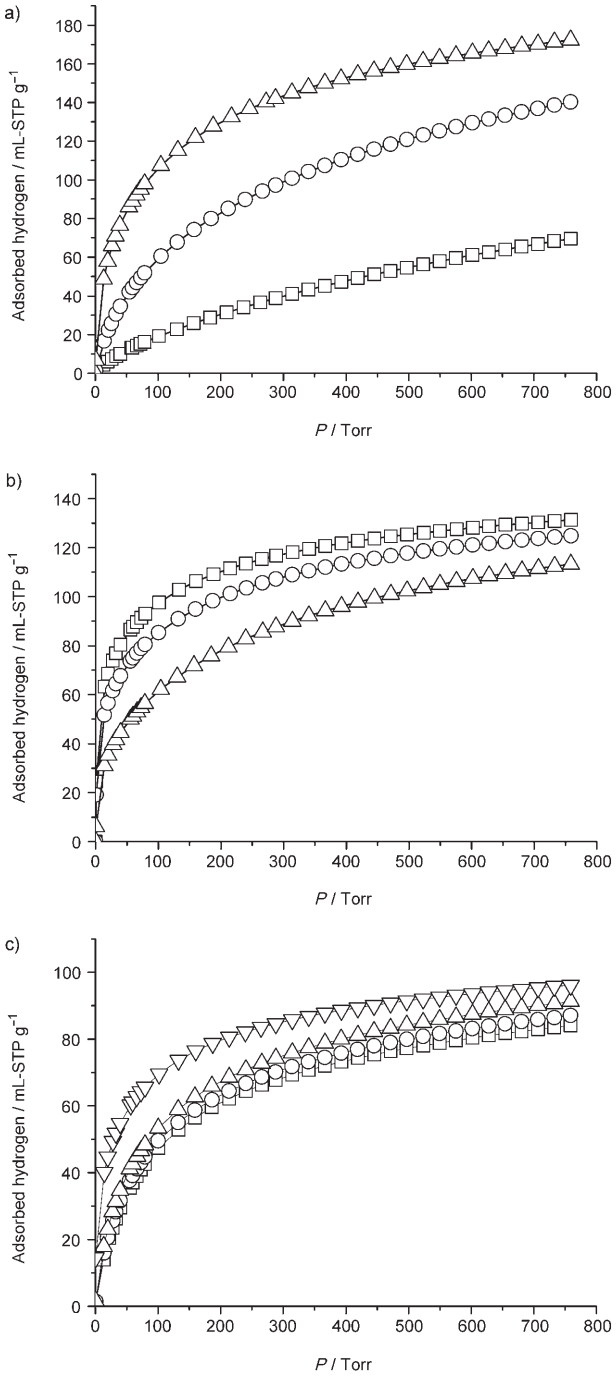

Figure 1. Hydrogen adsorption isotherms over zeolites with various Si/Al ratios at 77 K: a) △ FAU (2.81), ○ FAU (5.6), □ FAU (60); b) □ MOR (13), ○ MOR (20), △ MOR (90), and c) ▽ MFI (23), △ MFI (50), ○ MFI (80), □ MFI (140).

(Figure 4a) and three zeolites with similar Al concentrations (Figure 4b) when the adsorbed hydrogen is 30 mL g^{-1}. The $-\Delta H_{ads}$ can be obtained from the slopes of Figure 4 and the results are presented in Table 1. For other cases, including various hydrogen uptakes, zeolite structures and Al or Na concentration, $-\Delta H_{ads}$ values are obtained similarly, and the results are shown in Table 1 and Figure 5 for selected cases.

Table 1. Physicochemical properties of various zeolites and a summary of their hydrogen adsorption results.

Sample (SiO_2/Al_2O_3 ratio)	Al/(Al+Si) [%]	S_{BET}[a] [$m^2 g^{-1}$]	$PV\mu$[b] [$mL g^{-1}$]	H_2 adsorption[c] [mL-STP g^{-1}]	Surface coverage[d] [%]	Micropore volume occupancy[e] [%]	$P_{1/2}$[f] [Torr]	$-\Delta H_{ads}$[g] [kJ mol^{-1}]				
								20	25	30	35	40
FAU (2.81)	41.6	604	0.29	172	97.8	76.7	54.0	6.9	6.8	6.4	6.9	7.0
FAU (5.6)	26.3	827	0.39	140	55.5	45.8	140.0	6.1	6.0	6.0	6.0	5.8
FAU (60)	3.2	749	0.36	71	32.6	25.2	230.0	4.8	4.7	4.6	4.6	–
MOR (13)	13.3	425	0.19	131	105.9	86.1	16.4	11.7	10.9	9.2	6.6	6.7
MOR (20)	9.1	500	0.22	124	85.2	72.6	28.7	10.9	8.8	8.2	7.8	7.8
MOR (90)	2.2	500	0.24	113	77.6	59.1	80.2	7.2	7.5	7.6	7.6	7.2
MFI (23)	8.0	425	0.16	96	77.6	77.0	25.6	ND[h]	ND	ND	ND	ND
MFI (50)	3.9	425	0.20	91	73.5	56.9	68.7	6.7	6.7	6.7	6.6	6.6
MFI (80)	2.4	425	0.22	87	70.3	50.2	73.8	6.6	6.5	6.4	6.3	6.3
MFI (140)	1.4	425	0.21	84	67.9	50.1	77.4	6.3	6.2	6.2	6.2	6.2

[a] Surface area calculated by the BET equation. [b] Micropore volume calculated by the t-plot. [c] Adsorption capacity of hydrogen at 760 Torr. [d] Relative surface coverage based on the fact that 1.3×10^{-5} mol of adsorbed hydrogen is needed to cover (monolayer) one square meter of a solid surface. [e] Relative micropore occupancy by hydrogen calculated by using the density of liquid hydrogen (0.07 g mL^{-1}). [f] The pressure at which half of adsorption capacity (at 760 Torr) is adsorbed. [g] Heat of adsorption calculated by the Clausius–Clapeyron equation when the adsorbed amount is 20–40 mL g^{-1} [h] ND: not-determined.

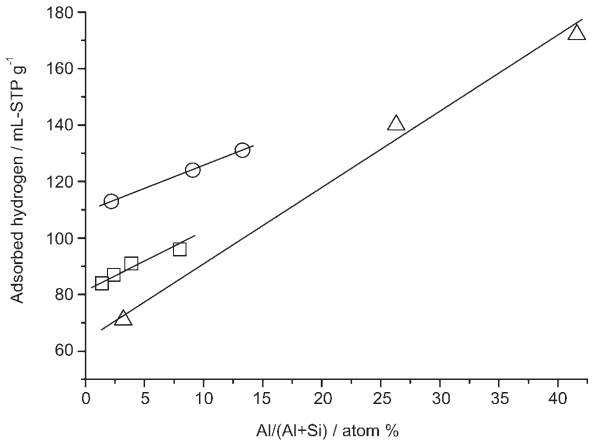

Figure 2. Effect of Al concentration of various zeolites on hydrogen adsorption capacities at 760 Torr. ○ MOR, □ MFI, △ FAU.

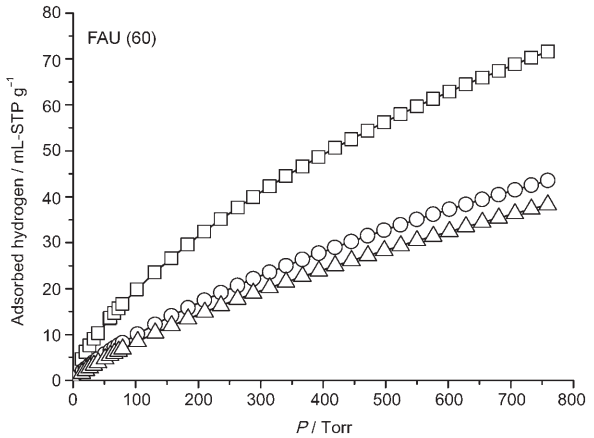

Figure 3. Effect of adsorption temperature on hydrogen adsorption on FAU (60) zeolite. □ 77 K, ○ 87 K, △ 90 K.

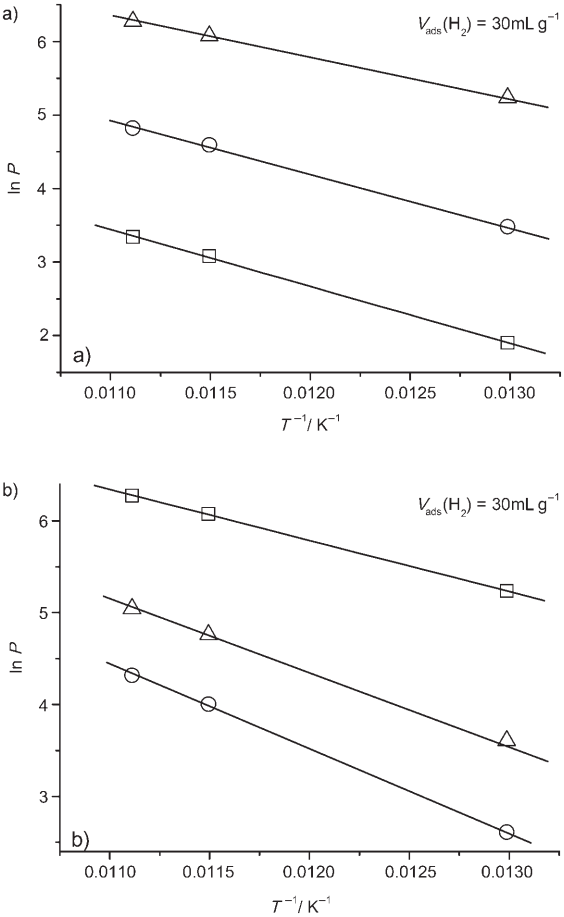

Figure 4. Clausius–Clapeyron plots over various zeolites: a) FAU zeolites with various Si/Al ratios. △ FAU (60), ○ FAU (5.6), □ FAU (2.81); b) FAU, MFI, and MOR zeolites with similar Si/Al ratios. □ FAU (60), △ MFI (80), ○ MOR (90).

As shown in Table 1 and Figure 5a, the isosteric heat of adsorption increases with increasing Al concentration for the three zeolites, illustrating that the interaction between hydrogen and zeolite pore walls (or cations) increases with Al concentration. Moreover, $-\Delta H_{ads}$ is in the order of MOR > MFI > FAU when the three zeolites have similar Al

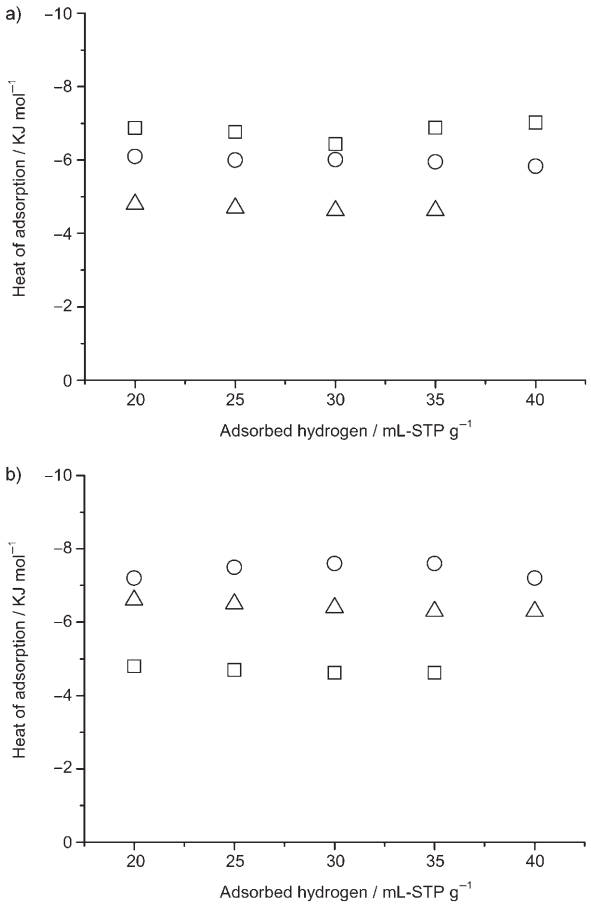

Figure 5. Isosteric heat of adsorptions over various zeolites for hydrogen adsorption of 20–40 mL g^{-1}: a) FAU zeolite with various Si/Al ratios. □ FAU (2.81), ○ FAU (5.6), △ FAU (60); b) FAU, MFI, and MOR zeolites with similar Si/Al ratios. □ FAU (60), ○ MOR (90), △ MFI (80).

concentrations (Table 1 and Figure 5b), suggesting that the interaction between hydrogen and zeolites is in the order of MOR > MFI > FAU. Therefore, hydrogen adsorption depends on not only the Al concentration but also zeolite structure.

Hydrogen uptake as a function of adsorption pressure varies considerably depending on the type of zeolites and Si/Al ratios. The normalized uptakes are shown in Figure 6 for faujasite zeolites. Other zeolites show similar dependences on the aluminum concentration. The differences are, however, rather small between samples of MFI (or MOR) with Si/Al ratios because of the relatively small difference in Al concentrations. The pressures ($P_{1/2}$) at which half of the total adsorption capacity at 760 Torr is adsorbed are summarized in Table 1. Hydrogen adsorbs readily into zeolite pores at a relatively low pressure with increasing aluminum (or sodium) concentration for the three zeolites, thus indicating an increase of interaction between hydrogen and the pores of the zeolites with increasing the electrostatic field due to the increase of aluminum and cation (sodium in this case). Compared with the FAU zeolites, the low $P_{1/2}$ for MOR or MFI zeolites confirms the strong interaction between hydrogen and the pores of MOR or MFI in accord with the high $-\Delta H_{ads}$ for the MOR and MFI zeolites.

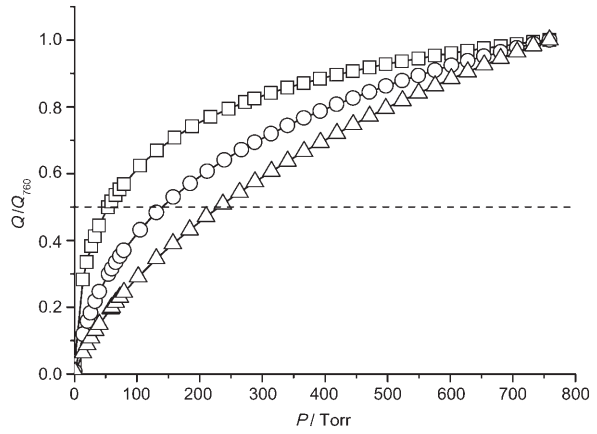

Figure 6. Hydrogen adsorption isotherms normalized to the adsorption capacity at 760 Torr over FAU zeolites with various Si/Al ratios. □ FAU (2.81), ○ FAU (5.6), △ FAU (60).

The relative surface coverage, meaning the fraction of surface area that is covered by hydrogen, was also calculated (Table 1) based on the fact that 1.3×10^{-5} mol of adsorbed hydrogen is needed to cover one square meter of an adsorbent by monolayer.[1] The relative surface coverage increases with increasing Al concentrations of zeolites (Table 1), which is consistent with the heat of adsorption. Moreover, in accord with the heat of adsorption, the surface coverage is in the order of MOR > MFI > FAU when the Al concentration is similar (Table 1 and Figure 7). In our previous study, it has been reported that the surface coverage on AlPOs increases with the decrease of pore size due to an increase of interaction between hydrogen and pore walls for small-pore AlPOs.[20] Therefore, the interaction between hydrogen and the pores of zeolites increases when the Al concentration is high, especially for the MOR zeolite. It is not certain as to whether the surface coverage higher than 100% means multilayer adsorption or not. We cannot rule out the experimental error even though the reproducibility

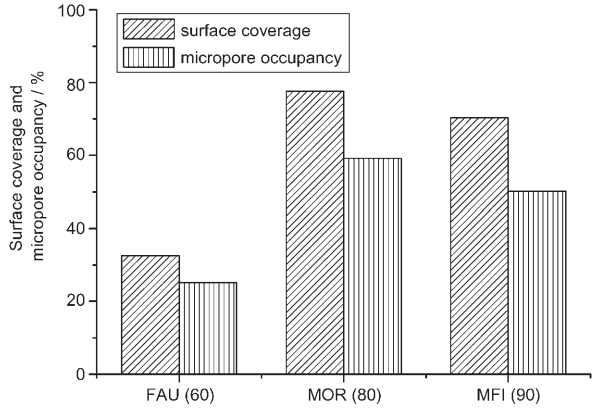

Figure 7. Surface coverages and micropore occupancies over FAU (60), MFI (90) and MOR (80) zeolites with similar Si/Al ratios.

of hydrogen adsorption is very high. The relative surface coverage is usually below 100% except for a porous hybrid material, manganese formate, for which the coverage is 150%.[33]

Micropore occupancy, calculated from the PV_{μ} and the volume of adsorbed hydrogen, shows very similar trends to those of surface coverage (Table 1 and Figure 7). As the aluminum concentration increases, the micropore occupancy increases for the three zeolites. The micropore occupancy is in the order of MOR > MFI > FAU when the aluminum (or sodium) concentration is similar (Table 1 and Figure 7). The micropore occupancies of adsorbed hydrogen on AlPOs, several MOFs, and porous zinc dicarboxylate diamines are 37–80,[20] 13–64,[21] and 37 −52%,[34] respectively.

Discussion

Aluminosilicate zeolites are well known for their electrostatic fields[35] due to the electronegitivity[36] differences between Al, Si, and O and the contribution of charge-balancing cations. As the Al concentration increases, the electrostatic field of a zeolite increases accordingly.[35] So far, the effect of the Si/Al ratio or electrostatic field on hydrogen adsorption has not been established conclusively.[25,30] We hypothesized that the electrostatic field may increase the adsorption capacity of hydrogen considerably at low pressure because coordinatively unsaturated sites (CUS) increase the adsorption strength due to the polarization of adsorbed hydrogen.[27,28] Very recently, Rowsell and Yaghi have also reported that CUS leads to an increased hydrogen uptake.[21] As shown in Figure 2, the adsorption capacity (at 760 Torr) increases with Al concentration irrespective of the zeolite types. Moreover, the isosteric heat of adsorption (Table 1 and Figure 5a), surface coverage (Table 1), micropore occupancy (Table 1), and $P_{1/2}$ (pressures at which half of the total adsorption capacity at 760 Torr is adsorbed; Table 1 and Figure 6) confirm the stronger interaction for a zeolite with a higher concentration of Al (also a higher sodium concentration) because of the higher electrostatic field. Very recently, Frost et al.,[37] by using Grand canonical Monte Carlo simulations, have shown that heat of adsorption is one of the most important factors for adsorption at low pressures, presumably because the interaction is very important at low pressure. We have also analyzed the effect of the electrostatic field by the adsorption on FAU zeolites that were ion-exchanged with alkali metals and alkali-earth metals. The results can be explained by means of the size of ions and electrostatic fields and will be reported elsewhere.

We also analyzed the adsorption for the three zeolites (FAU (60), MOR (90), and MFI (80)) with similar Al concentrations to understand the effect of pore structures. The adsorption capacity (Table 1), $-\Delta H_{ads}$ (Figure 5b), surface coverage, and micropore occupancy (Figure 7) increase in the order of FAU < MFI < MOR. The $P_{1/2}$, however, decreases in the order of FAU > MFI ≈ MOR. All these results confirm that the strength of interaction between hydrogen and the pore wall of a zeolite is in the order of FAU < MFI < MOR. Very recently, we have shown that the heat of adsorption and adsorption capacity (per unit micropore volume or BET surface area) increase when decreasing the pore size of AlPOs.[20] In addition, AlPOs with smaller pore sizes favorably adsorb hydrogen at relatively low pressures.[20] FAU and MFI are composed of three-dimensional (3D) channels delineated by 12 and 10-membered rings (MR), respectively.[31] The two zeolites have intersections formed by the crossing channels.[31] On the contrary, the MOR is composed of an one-dimensional (1D) channel (12MR) without intersection.[31] Pore sizes of FAU, MFI, and MOR are $0.74 \times 0.74 \times 0.51 \times 0.55$ nm (or 0.53×0.56 nm) and 0.7×0.65 nm, respectively.[31] From the adsorption results and our experience, it may be concluded that the effectiveness of pore structure of zeolites for hydrogen adsorption decreases in the order of MOR > MFI > FAU. The effective adsorption on MOR might be related with the 1D channel structure without intersections. The inefficient hydrogen storage over FAU is probably due to the larger pore structure and larger intersection.

Conclusion

In this work, we have demonstrated unequivocally that the adsorption capacity, the isosteric heat of adsorption ($-\Delta H_{ads}$), surface coverage, and micropore occupancy increase with increasing Al or Na concentration of zeolites irrespective of framework structures. Moreover, the adsorption capacity, surface coverage, micropore occupancy, and the heat of adsorption over three zeolites with similar Al or Na concentration increase in the order of FAU < MFI < MOR. The hydrogen adsorbs readily at relatively low pressure for porous materials containing high concentrations of Al or with the structure of the MOR zeolite. Therefore, it is reasonable to suggest that the ideal zeolite for an efficient hydrogen storage, especially at low pressure, is one with higher concentrations of Al or Na (to show high electrostatic field) and narrow pores without intersections.

Experimental Section

General methods: Several zeolites, such as faujasite, mordenite, and ZSM-5 were obtained from Zeolyst (faujasite and ZSM-5) or Zeocat (mordenite). Zeolites in ammonium or proton forms were fully ion-exchanged into sodium form by a conventional ion-exchange method by using aqueous NaCl solution (three exchanges). The zeolites are denoted as FAU (*n*), MOR (*n*), or MFI (*n*) in which *n* means the SiO_2/Al_2O_3 ratio of the zeolite. The specifications of zeolites used in this study are summarized in Table 1. FAU (60), MOR (90), and MFI (80) were used to study the effect of pore structure because the three zeolites have similar Al/(Si+Al) atomic ratios of 2.2–3.2%.

The surface area and micropore volume of various zeolites were calculated from nitrogen adsorption isotherms by using the BET equation and the t-plot, respectively. The nitrogen adsorption isotherms were obtained by using a Micromeritics ASAP 2400 adsorption unit at liquid nitrogen temperature after evacuation under vacuum. The H_2 adsorption on vari-

ous zeolites was also conducted by using a volumetric adsorption apparatus (Tristar 3300, Micrometrics) at liquid nitrogen (77 K), liquid argon (87 K), and liquid oxygen temperature (90 K). The adsorption capacities at various pressures were calculated by using the ideal gas law because the adsorption pressure was only up to 760 Torr. The accuracy of the adsorption unit for the measurement of the adsorption capacity was confirmed by conducting the experiments on the well-known molecular sieves, such as K-Y and SAPO-34. The reproducibility of the adsorption data was confirmed at least three times, and the experimental error of the adsorption capacity was less than 2 $mL\,g^{-1}$ at 760 Torr. The results shown in this study are averaged results derived from three or four independent experiments.

The isosteric heat of adsorption ($-\Delta H_{ads}$) was calculated by using the Clausius–Clapeyron equation[32] from the adsorption isotherms at three temperatures. The Clausius–Clapeyron equation is expressed as

$$\ln P = -\Delta H_{ads} R^{-1} T^{-1} \quad (1)$$

in which, P, R, and T are the pressure, gas constant, and temperature, respectively. The $-\Delta H_{ads}$ can be obtained from the slope of the plot of Equation (1). The surface coverage was calculated based on the fact that 1.3×10^{-5} mol of adsorbed hydrogen is needed to cover one square meter of an adsorbent by monolayer.[1] The micropore occupancy was obtained from the volume of adsorbed hydrogen (calculated with the density of liquid hydrogen of 0.07 $g\,mL^{-1}$) and micropore volume of a zeolite.

Acknowledgements

This work was supported by Institutional Research Program (KK-0703-E0). The authors wish to thank Dr. S. M. Humphrey (Cambridge University, UK), Dr. P. M. Forster (Stony Brook University, USA), Dr. J. Eckert (University of California, Santa Barbara, USA), Dr. Y. K. Hwang (KRICT, Korea), Dr. D. P. Amalnerkar (C-MET, India), and Dr. A. S. Mamman (NCL, India) for helpful discussions. We also thank Miss H.-K. Kim of KRICT for her experimental assistance.

[1] L. Schlapbach, A. Züttel, *Nature* **2001**, *414*, 353.
[2] A. M. Seayad, D. M. Antonelli, *Adv. Mater.* **2004**, *16*, 765.
[3] A. Züttel, *Mater. Today* **2003**, *6*, 24.
[4] F. L. Darkrim, P. Malbrunot, G. P. Tartaglia, *Int. J. Hydrogen Energy* **2002**, *27*, 193.
[5] A. C. Dillon, M. J. Heben, *Appl. Phys. A* **2001**, *72*, 133.
[6] R. Ströbel, J. Garche, P. T. Moseley, L. Jörissen, G. Wolf, *J. Power Sources* **2006**, *159*, 781.
[7] a) C. O. Arean, G. T. Palomino, E. Garrone, D. Nachtigallova, P. Nachtigall, *J. Phys. Chem. B* **2006**, *110*, 395; b) A. Zecchina, S. Bordiga, J. G. Vitillo, G. Ricchiardi, C. Lamberti, G. Spoto, M. Bjørgen, K. P. Lillerud, *J. Am. Chem. Soc.* **2005**, *127*, 6361.
[8] a) J. Eckert, J. M. Nicol, J. Howard, F. R. Trouw, *J. Phyc. Chem.* **1996**, *100*, 10646; b) M. G. Nijkamp, J. E. M. J. Raaymakers, A. J. van Dillen, K. P. de Jong, *Appl. Phys. A* **2001**, *72*, 619; c) A. J. Ramirez-Cuesta, P. C. H. Mitchell, *Catal. Today* **2007**, *120*, 368.
[9] J. L. C. Rowsell, O. M. Yaghi, *Angew. Chem.* **2005**, *117*, 4748; *Angew. Chem. Int. Ed.* **2005**, *44*, 4670.
[10] a) G. Férey, M. Latroche, C. Serre, F. Millange, T. Loiseau, A. Percheron-Guégan, *Chem. Commun.* **2003**, 2976; b) E. Y. Lee, M. P. Suh, *Angew. Chem.* **2004**, *116*, 2858; *Angew. Chem. Int. Ed.* **2004**, *43*, 2798; c) B. Kesanli, Y. Cui, M. R. Smith, E. W. Bittner, B. C. Bockrath, W. Lin, *Angew. Chem.* **2005**, *117*, 74; *Angew. Chem. Int. Ed.* **2005**, *44*, 72.
[11] a) B. Panella, M. Hirscher, H. Pütter, U. Müller, *Adv. Funct. Mater.* **2006**, *16*, 520; b) B. Chen, N. W. Ockwig, A. R. Millward, D. S. Contreras, O. M. Yaghi, *Angew. Chem.* **2005**, *117*, 4823; *Angew. Chem. Int. Ed.* **2005**, *44*, 4745..
[12] J. L. C. Rowsell, E. C. Spencer, J. Eckert, J. A. K. Howard, O. M. Yaghi, *Science* **2005**, *309*, 1350.
[13] J. L. C. Rowsell, A. R. Millward, K. S. Park, O. M. Yaghi, *J. Am. Chem. Soc.* **2004**, *126*, 5666.
[14] S. H. Jhung, J. W. Yoon, H.-K. Kim, J.-S. Chang, *Bull. Korean Chem. Soc.* **2005**, *26*, 1075.
[15] A. G. Wong-Foy, A. J. Matzger, O. M. Yaghi, *J. Am. Chem. Soc.* **2006**, *128*, 3494.
[16] M. Latroche, S. Surblé, C. Serre, C. Mellot-Draznieks, P. L. Llewellyn, J.-H. Lee, J.-S. Chang, S. H. Jhung, G. Férey, *Angew. Chem.* **2006**, *118*, 8407; *Angew. Chem. Int. Ed.* **2006**, *45*, 8227.
[17] M. Dincã, A. Dailly, Y. Liu, C. M. Brown, D. A. Neumann, J. R. Long, *J. Am. Chem. Soc.* **2006**, *128*, 16876.
[18] M. Dinca, J. R. Long, *J. Am. Chem. Soc.* **2005**, *127*, 9376.
[19] P. Pan, M. B. Sander, X. Huang, J. Li, M. Smith, E. Bittner, B. Bockrath, J. K. Johnson, *J. Am. Chem. Soc.* **2004**, *126*, 1308.
[20] S. H. Jhung, H.-K. Kim, J. W. Yoon, J.-S. Chang, *J. Phys. Chem. B* **2006**, *110*, 9371.
[21] J. L. C. Rowsell, O. M. Yaghi, *J. Am. Chem. Soc.* **2006**, *128*, 1304.
[22] a) Y. Li, R. T. Yang, *J. Am. Chem. Soc.* **2006**, *128*, 726; b) Y. Li, R. T. Yang, *J. Am. Chem. Soc.* **2006**, *128*, 8136.
[23] X. Zhao, B. Xiao, A. Fletcher, K. M. Thomas, D. Bradshaw, M. J. Rosseinsky, *Science* **2004**, *306*, 1012.
[24] D. Sun, S. Ma, Y. Ke, D. J. Collins, H.-C. Zhou, *J. Am. Chem. Soc.* **2006**, *128*, 3896.
[25] V. B. Kazansky, V. Yu. Borovkov, A. Serich, H. G. Karge, *Microporous Mesoporous Mater.* **1998**, *22*, 251.
[26] G. E. Froudakis, *Nano Lett.* **2001**, *1*, 531.
[27] P. M. Forster, J. Eckert, J.-S. Chang, S.-E. Park, G. Férey, A. K. Cheetham, *J. Am. Chem. Soc.* **2003**, *125*, 1309.
[28] P. M. Forster, J. Eckert, B. D. Heiken, J. B. Parise, J. W. Yoon, S. H. Jhung, J.-S. Chang, A. K. Cheetham, *J. Am. Chem. Soc.* **2006**, *128*, 12846.
[29] Q. Yang, C. Zhong, *J. Phys. Chem. B* **2006**, *110*, 655.
[30] H. W. Langmi, M. M. Al-Mamouri, S. R. Johnson, D. Book, J. D. Speight, P. P. Edwards, I. Gameson, P. A. Anderson, I. R. Harris, *J. Alloys Compd.* **2003**, *356–357*, 710.
[31] IZA (international zeolite association) code and structure of a zeolite can be retrieved in a web site of http://www.iza-structure.org/databases/
[32] J. M. Thomas, W. J. Thomas, *Introduction to the Principles of Heterogeneous Catalysis*, **1967**, Academic Press, New York.
[33] D. N. Dybtsev, H. Chun, S. H. Yoon, D. Kim, K. Kim, *J. Am. Chem. Soc.* **2004**, *126*, 32.
[34] H. Chun, D. N. Dybtsev, H. Kim, K. Kim, *Chem. Eur. J.* **2005**, *11*, 3521.
[35] a) D. W. Breck, *Zeolite Molecular Sieves*, **1974**, Wiley, New York; b) E. Preuss, G. Linden, M. Peuckert, *J. Phys. Chem.* **1985**, *89*, 2955.
[36] Pauling's electronegativity of Al, Si, and O is 1.61, 1.90, and 3.44, respectively.
[37] H. Frost, T. Düren, R. Q. Snurr, *J. Phys. Chem. B* **2006**, *110*, 9565.

Received: January 29, 2007
Published online: May 11, 2007

